THE JOURNAL OF BIOLOGICAL CHEMISTRY VOL. 286, NO. 7, pp. 5494–5505, February 18, 2011

Splice Variants of the Dual Specificity Tyrosine Phosphorylation-regulated Kinase 4 (DYRK4) Differ in Their Subcellular Localization and Catalytic Activity*[S]

Received for publication, June 24, 2010, and in revised form, December 1, 2010 Published, JBC Papers in Press, December 2, 2010, DOI 10.1074/jbc.M110.157909

Chrisovalantis Papadopoulos[‡§], Krisztina Arato[‡¶1], Eva Lilienthal[§], Johannes Zerweck[‖], Mike Schutkowski[‖], Nicolas Chatain[‡‡], Gerhard Müller-Newen[‡‡], Walter Becker[§], and Susana de la Luna[‡¶§§2]**

*From the [‡]Genes and Disease Program, Centre for Genomic Regulation, University Pompeu Fabra, Dr. Aiguader 88, 08003 Barcelona, Spain, the [§]Institute of Pharmacology and Toxicology, Rheinisch-Westfaelische Technische Hochschule Aachen University, Wendlingweg 2, 52074 Aachen, Germany, the [¶]Centro de Investigación Biomédica en Red de Enfermedades Raras, 08003 Barcelona, Spain, the [‡‡]Department of Biochemistry, Rheinisch-Westfaelische Technische Hochschule Aachen University, Pauwelsstrasse 30, 52074 Aachen, Germany, [‖]JPT Peptide Technologies GmbH, Volmerstrasse 5, 12489 Berlin, Germany, the **Institute of Biochemistry and Biotechnology, University of Halle-Wittenberg, Kurt-Mothes Strasse 3, 06099 Halle (Saale), Germany, and the [§§]Institució Catalana de Recerca i Estudis Avançats, 08003 Barcelona, Spain*

Dual specificity tyrosine phosphorylation-regulated kinases, DYRKs, are a family of conserved protein kinases that play key roles in the regulation of cell differentiation, proliferation, and survival. Of the five mammalian DYRKs, DYRK4 is the least studied family member. Here, we show that several splice variants of DYRK4 are expressed in tissue-specific patterns and that these variants have distinct functional capacities. One of these variants contains a nuclear localization signal in its extended N terminus that mediates its interaction with importin α3 and α5 and that is capable of targeting a heterologous protein to the nucleus. Consequently, the nucleocytoplasmic mobility of this variant differs from that of a shorter isoform in live cell imaging experiments. Other splicing events affect the catalytic domain, including a three-amino acid deletion within subdomain XI that markedly reduces the enzymatic activity of DYRK4. We also show that autophosphorylation of a tyrosine residue within the activation loop is necessary for full DYRK4 kinase activity, a defining feature of the DYRK family. Finally, by comparing the phosphorylation of an array of 720 peptides, we show that DYRK1A, DYRK2, and DYRK4 differ in their target recognition sequence and that preference for an arginine residue at position P −3 is a feature of DYRK1A but not of DYRK2 and DYRK4. Therefore, we highlight the use of subcellular localization as an important regulatory mechanism for DYRK proteins, and we propose that substrate specificity could be a source of functional diversity among DYRKs.

Dual specificity tyrosine phosphorylation-regulated kinases (DYRKs)[3] are members of an evolutionarily conserved family of protein kinases that play key roles in the regulation of cell differentiation, proliferation, and survival (1, 2). DYRKs share a conserved kinase domain and adjacent N-terminal DYRK homology (DH)-box, although they differ in their N- and C-terminal extensions (3). From a phylogenetic point of view, DYRKs are divided into two subclasses that can be identified through the presence of specific protein motifs (2). Class I DYRKs harbor a functional, bipartite nuclear localization signal (NLS) N-terminal to the DH-box, and a C-terminal PEST or GAS region. This class includes the *Drosophila* minibrain kinase (*mnb*), *Caenorhabditis elegans* MBK-1, and mammalian DYRK1A and DYRK1B (4–6). Class II DYRKs do not present any known protein domain within the N- and C-terminal extensions, except for the NAPA domain N-terminal to the DH-box (7), and they include mammalian DYRK2, DYRK3, and DYRK4, *Drosophila* dDYRK2 (*smi35*), *C. elegans* MBK-2 and *Schizosaccharomyces pombe* Pom1p (4, 5, 8, 9).

DYRKs contain a conserved Tyr-Xaa-Tyr motif in the activation loop, and the phosphorylation of the second tyrosine residue is essential for full catalytic activity of all the DYRKs tested to date (2, 10). Using dDYRK2 as a model, it has been shown that this critical tyrosine residue is autophosphorylated during translation (11), although notably, mature DYRKs only phosphorylate substrates on serine or threonine residues. The definition of a consensus phosphorylation sequence for DYRK1A, RP*X*(S/T)P (12), has stimulated the identification of numerous phosphorylation sites in DYRK1A substrates (2). Some DYRK1A substrates, such as eukaryotic initiation factor 2Bϵ, the microtubule-associated protein Tau, or glycogen synthase are also phosphorylated by DYRK2 *in vitro* (13, 14), whereas histone H2B is only phosphorylated by DYRK2 and DYRK3 but not by DYRK1A (4). A comparative

* This work was supported by Spanish Ministry of Science and Innovation Grant BFU2007-61043 and BFU2010-15347 (to S. L.), Departament d'Innovació, Universitats i Empresa de la Generalitat de Catalunya Grant 2009SGR1464 (to S. L.), Deutsche Forschungsgemeinschaft SFB 542, Projects B12 and Z1 (to G. M.-N.) and BE-1967/2-1 (to W. B.), and the German Academic Exchange Service DAAD doctoral fellowship (to C. P.).

[S] The on-line version of this article (available at http://www.jbc.org) contains supplemental Figs. S1–S8, Tables S1–S4, "Experimental Procedures," and videos 1 and 2.

[1] Formación del Profesorado Universitario predoctoral fellow (Spanish Ministry of Education).

[2] To whom correspondence should be addressed: Centre de Regulació Genòmica-CRG, Dr. Aiguader 88, 08003 Barcelona, Spain. Tel.: 34-93-316-0144; Fax: 34-93-316-0088; E-mail: susana.luna@crg.es.

[3] The abbreviations used are: DYRK, dual specificity tyrosine phosphorylation-regulated kinase; DH, DYRK homology; NLS, nuclear localization signal; ROI, region of interest; FLIP, fluorescence loss in photobleaching; IVK, *in vitro* kinase; EST, expressed sequence tag.

analysis of peptide substrates has also revealed both similarities and differences in the substrate specificity of DYRK1A and DYRK2 or DYRK3 (15). However, the substrate specificities of different members of the DYRK family have not yet been systematically compared.

Because no activating kinase appears to be required, other control mechanisms may regulate the biological activity of DYRKs. Indeed, the subcellular localization of DYRKs has emerged as one such mechanism. Yeast Yak1p translocates to the nucleus in response to glucose availability (16), and changes in MBK-2 localization from the cortex to the cytoplasm have been described during *C. elegans* zygote maturation (17). DYRK1B accumulates in the cytosol of cells from rhabdomyosarcoma tumors, although it is predominantly found in the nucleus of undifferentiated NIH-3T3 cells (18), and DYRK2 has been shown to translocate to the nucleus upon genotoxic stress (19).

Among the mammalian class II DYRKs, DYRK2 and DYRK3 are most closely related, and they are encoded by paralogous genes that originated by gene duplication (20). Despite this close relationship, they have acquired very different functions. DYRK2 is involved in the response to DNA damage through p53 phosphorylation (19), whereas DYRK3 regulates erythropoiesis through as yet unknown molecular pathways (21, 22). In contrast to DYRK2 and DYRK3, very little is known about the function of the other mammalian class II DYRK, DYRK4, and no substrate has been identified for this kinase. Rat and murine DYRK4s were reported to be testis-specific kinases expressed only in stage VIII post-meiotic spermatids (4, 23). However, *Dyrk4*-deficient mice are fertile (23), which could possibly reflect some redundancy in function of the class II DYRKs, all of which are strongly expressed in the testis. Conversely, it remains unclear whether DYRK4 can phosphorylate the same substrates as other DYRKs and thus substitute for a loss of DYRK3 or DYRK2.

In this study, we aimed to comprehensively characterize the expression of DYRK4 in human tissues, as well as its subcellular localization, catalytic properties, and substrate specificity. We found that, in contrast to the rat and mouse orthologues, human DYRK4 is widely expressed. Alternative splicing generates several DYRK4 isoforms; some of the splicing events affect the subcellular localization, whereas others result in distinct kinase activities. In addition, we show that autophosphorylation of the second tyrosine residue within the activation loop is necessary for full activity of DYRK4. Finally, we show that DYRK1A, DYRK2, and DYRK4 differ in their substrate specificities and that class II DYRKs (DYRK2 and DYRK4) are less biased than class I DYRK1A toward peptides with an arginine at position P −3.

EXPERIMENTAL PROCEDURES

Plasmids—Details on the generation of all the plasmids used in this study, as well as the sequences of the oligonucleotides used, are provided in the supplemental "Experimental Procedures".

Fluorescence Microscopy and Shuttling Analysis—The conditions for transfection and cell growth of the cells on coverslips are provided in supplemental "Experimental Procedures". To detect green fluorescent protein (GFP)-tagged proteins in the transfected cells, they were first fixed in 4% paraformaldehyde in phosphate-buffered saline (PBS) for 15 min at room temperature. The coverslips were then mounted in Vectashield (Vector Laboratories) containing 500 ng/ml 4′,6-diamidino-2-phenylindole (DAPI), and they were analyzed under a Zeiss Observer.Z1, and images were acquired with an AxioCam MRm camera.

Confocal imaging and the fluorescence loss in photobleaching (FLIP) assays were performed using a Zeiss LSM 510 Meta confocal microscope equipped with an argon laser. Cells were examined with a 63 × 1.2 NA Zeiss water immersion objective. GFP was excited at $\lambda = 488$ nm and detected using a 505–530 bandpass filter. Yellow fluorescent protein (YFP) was excited at $\lambda = 514$ nm and using a 530–600 bandpass filter. In the FLIP assay, bleaching was performed with 14 pulses each consisting of 50 iterations in a cytoplasmic region of interest (ROI) until most of the cytoplasmic fluorescent protein was bleached. Data were recorded after each bleach pulse and subsequently every 30 s. Four ROIs were used to measure the fluorescence intensities. The first ROI was taken from the bleached region (ROI) and a second ROI from the nucleus (Nuc) of the bleached cell. A third ROI was taken from a non-bleached neighboring cell to measure the loss of fluorescence during image acquisition (Con), and the fourth ROI was monitored the background (BG) fluorescence. Normalized fluorescence intensities were calculated from five representative FLIP measurements as follows: 1) background subtraction: ROI (t) − BG (t), Nuc (t) − BG (t), Con (t) − BG (t); 2) correction: (ROI (t) − BG (t))/(Con (t) − BG (t)), (Nuc (t) − BG (t))/(Con (t) − BG (t)); 3) normalization: ((ROI (t) − BG (t))/(Con (t) − BG (t)))·((ROI (0) − BG (0))/(Con (0) − BG (0)).

Immunoprecipitation and Pulldown—Transfected cells were washed twice in cold PBS and lysed in buffer A (50 mM Hepes, pH 7.4, 150 mM NaCl, 0.1 mM EGTA, 1% Igepal, supplemented with 1 mM $NaVO_4$, 1 mM phenylmethylsulfonyl fluoride, 10 μg/ml aprotinin, 10 μg/ml pepstatin, and 10 μg/ml leupeptin). After centrifugation, the supernatant was obtained and incubated with 1 μg/sample of rabbit anti-GFP (Rockland) or mouse monoclonal anti-HA (Covance) for 1 h at 4 °C. Equilibrated EZview protein G affinity gel (Sigma) was added to each sample and incubated for 2 h at 4 °C, and the gel was then washed twice with washing buffer (50 mM Tris-HCl, pH 7.5, 150 mM NaCl, 2 mM EDTA and 0.1% Igepal) and twice with washing buffer without Igepal. The samples recovered were analyzed in Western blots (as described in supplemental "Experimental Procedures") or in *in vitro* kinase assays (as described below). Glutathione *S*-transferase (GST) pulldowns were performed as described previously (24).

In Vitro Kinase Assays—The *in vitro* kinase assays (IVK) were performed with either immunocomplexes from transfected cells or with bacterially expressed recombinant GST fusion proteins. Bacterially expressed GST-DYRK1A, GST-DYRK1A$^{\Delta C}$, or GST-DYRK2 were prepared as described previously (4, 12, 24). GST-DYRK4 proteins were expressed by inducing transformed *Escherichia coli* BL21(DE3)pLysS with 0.1 mM isopropyl β-D-1-thiogalactopyranoside for 4–6 h at 20 °C. Recombinant human GST-DYRK4 expressed in insect

cells (Invitrogen) was used for the peptide assay shown in Figs. 6 and 7*B*. One unit of DYRK activity was the amount that catalyzed the phosphorylation of 1 nmol of the synthetic peptide DYRKtide (at 100 μM, RRRFRPASPLRGPPK; see Ref. 12) in 1 min at 30 °C (25). For IVK assays from mammalian cells, immunocomplexes were incubated for 30 min at 30 °C in 20 μl of kinase buffer (25 mM Hepes, pH 7.4, 5 mM $MgCl_2$, 0.5 mM DTT), with a final concentration of 10 μM ATP and [γ-^{33}P]ATP (100–150 mCi/pmol) and with 100 μM of peptide where necessary. Incorporation of ^{33}P into DYRKtide and SAPtide (RRARKLTATPTPLGG) was determined in triplicate by dotting aliquots of the reaction mixture onto Whatman P-81 ion exchange paper, washing in 5% phosphoric acid, and counting by liquid scintillation. Incorporation of ^{33}P into Pep285 (Biotin-Ttds-VGLLKLASPELER, JPT Peptide Technologies) and Pep3 (Biotin-Ttds-TPGSRSRTPSLPT, JPT Peptide Technologies) was determined by dotting aliquots of the reaction onto a SAM^2 biotin capture membrane (Promega), washing twice in 2 M NaCl for 2 min, twice in 2 M NaCl in phosphoric acid for 3 min, twice in H_2O for 30 s, once in ethanol for 30 s and subsequently counting by liquid scintillation. To ensure equal expression of the fusion proteins and autophosphorylation, the kinases were eluted from the beads and analyzed in Western blots by autoradiography, and the absolute counts/min were normalized to the intensity of the signal in the immunoblots. For GST fusion proteins, eluted proteins (50 ng) were incubated for 20 min at 30 °C in 50 μl of kinase buffer with 50 μM ATP and [γ-^{32}P]ATP (1×10^{-3} μCi/pmol). Reactions were stopped by adding Laemmli sample buffer, and the samples were resolved by SDS-PAGE. The gels were stained with Coomassie Blue and dried, and ^{32}P incorporation was detected by autoradiography.

Phosphosite Array Screening—Peptide microarrays displaying phosphosite-derived peptides were prepared as described previously (26). Briefly, 720 13-mer peptides derived from known phosphorylation sites in human proteins were printed in triplicate onto aldehyde-modified glass slides. Two peptide chips were incubated with the reaction mixture face to face, with parafilm spacers placed at both ends. The reaction was allowed to proceed for 2 h at 30 °C in a total volume of 0.3 ml in kinase buffer with 1 μM [γ-^{33}P]ATP (150 μCi), 0.5 mg/ml bovine serum albumin, and 0.5–1 unit of the recombinant kinases. The slides were washed 15–20 times in 5% phosphoric acid and then with water and ethanol. The phosphorylated peptides were detected using a Storm 820 phosphorimager (GE Healthcare) at a resolution of 50 μm. The data were corrected for the background using local ring algorithm implemented in the software package ArrayPro Analyzer 4.0 (Media Cybernetics). False-positive signals due to irregularities such as air bubbles or spots were eliminated by comparison of the individual subarrays within the microarrays and by visual inspection. Only peptides exceeding a threshold intensity of 20% of the strongest signal on the array were considered positive. None of the peptides positive for any of the three kinases was phosphorylated by a kinase-negative mutant of GST-DYRK1A^{K188R} (data not shown).

Reverse Transcriptase and PCR Analysis—Total RNA from cell lines was isolated using the NucleoSpin RNA II kit (Macherey-Nagel) and subjected to reverse transcription using an oligo(dT)$_{12-18}$ primer and Superscript II reverse transcriptase (Invitrogen). A panel of human cDNAs normalized to the expression of housekeeping genes was purchased from Clontech (Human MTC Panel I). The sequences of the oligonucleotides used for the specific detection of DYRK4 splice variants are provided in supplemental Table S1. PCRs were performed with the GoTaq DNA polymerase (Promega), and the identity of the PCR products was verified by DNA sequencing.

RESULTS

Human and Murine DYRK4 Are Expressed as Multiple Alternative Splicing Variants—Data base mining indicates that at least two different murine *Dyrk4* transcripts exist (Fig. 1*A* and supplemental Fig. S1*A*). One of them encodes a protein product of 594 amino acids (mDYRK4^{594}, corresponding to accession number NM_207210), whereas the other (accession number AK077117) has a different 5′-terminal sequence and encodes a protein of 632 amino acids. Similarly, two different human DYRK4 protein products can be predicted as follows: a 520-amino acid protein described previously (hDYRK4^{520}, translated from accession number NM_003845; see Ref. 23) and a 635-amino acid protein (hDYRK4^{635}, translated from accession number AK308260; supplemental Fig. S1*B*). The existence of human *DYRK4* transcripts with different 5′-ends was confirmed by RT-PCR and sequencing of the PCR products (Fig. 1*C*). This analysis identified an alternative splicing event that involved the inclusion of an extra exon (exon 6 in humans; exon 3 in mice), which leads to a 9/10 amino acid inclusion in the human/murine DYRK4 proteins (Fig. 1, *B* and *C*), and would give rise to a protein isoform of 644/642 amino acids (hDYRK4^{644} and mDYRK4^{642}).

The N-terminal region of the long murine and human DYRK4 isoforms is encoded by orthologous exons (Fig. 1, *A* and *B*, and supplemental Figs. S1 and S2). In contrast, the short isoform of mouse *Dyrk4* starts with a 5′-exon that is not conserved in human *DYRK4* (Fig. 1*A*). We suggest that the longer isoform could be considered as the reference sequence for DYRK4, because the additional N-terminal sequence is conserved in mammals (Fig. 1*D*). By contrast, the corresponding first exon of the short variants appears to be species-specific, at least in human and mouse.

The analysis of several other human *DYRK4* transcripts obtained by RT-PCR, by sequencing of IMAGE clones or collected from databases, revealed further alternative splicing events. In the first place, exclusion of exon 18 leads to a frameshift and the generation of a protein with a truncated kinase domain, which would be predicted to lack activity (supplemental Figs. S3*B* and S4, *C–E*). Indeed, although the number of clones examined was small, exclusion of exon 18 appears to be more often represented in libraries from tumor tissue (supplemental Table S2). In addition, the use of an alternative splice donor site in exon 19 leads to the inclusion/exclusion of three amino acids (CLV) in the kinase subdomain XI (Fig. 5*A*, supplemental Fig. S2, and supplemental Table S2), an event also observed in murine *Dyrk4* (present in AK077117 and absent in NM_207210). Finally, an alternative acceptor site in exon 21 is responsible for the inclusion/exclu-

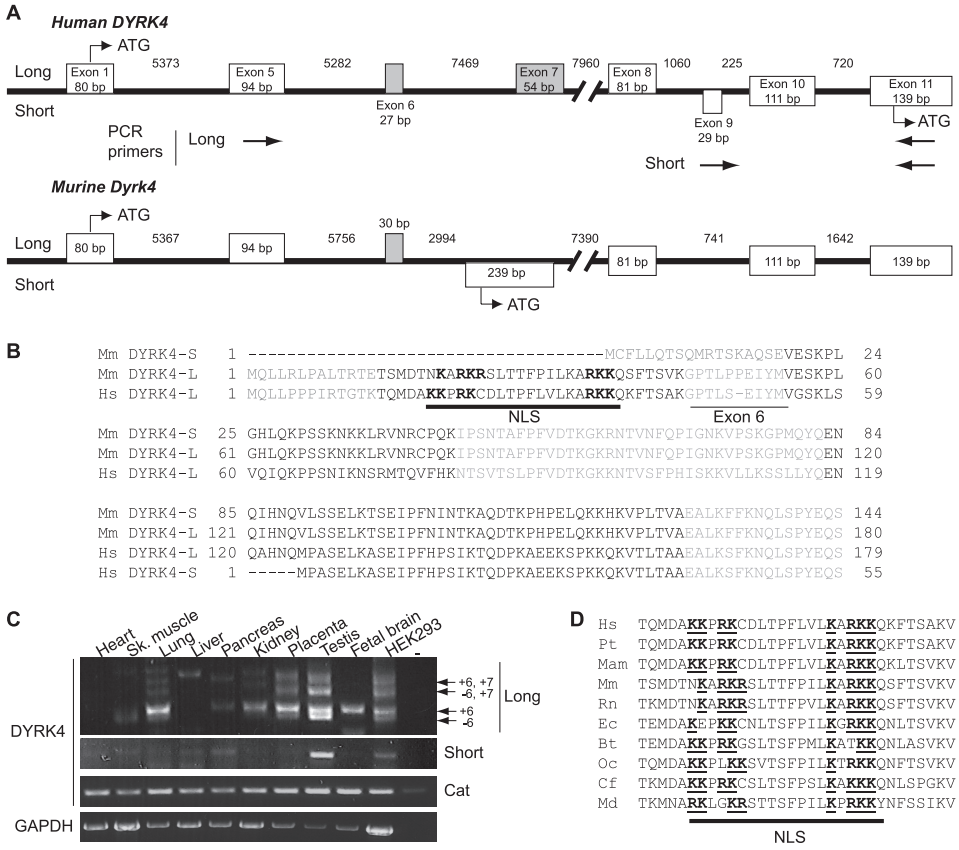

FIGURE 1. **Differential expression of DYRK4 isoforms.** *A,* schematic representation of the exon-intron structure of the 5′ end of the human and murine *DYRK4* gene. Exons are indicated by *boxes,* and the translation start point of the different isoforms is marked (*ATG*). The length of the exons and introns (in bp) was determined using either the Ensembl or University of California Santa Cruz (UCSC) servers. Additional alternatively spliced exons between exon 1 and exon 5 in the human gene are shown in supplemental Fig. S1. The alternatively spliced exons are *shaded*. The position of the PCR primers in *D* is indicated. *B*, alignment of the N-terminal regions of human (*Hs*) and murine (*Mm*) DYRK4. Translation of the different exons is shown in alternating colors (*black* and *gray*), and the alternatively spliced exon 6/3 is *underlined*. A predicted bipartite NLS is shown (*bold underlined*), and the basic amino acid residues are highlighted in *bold*. *C*, differential expression of *DYRK4* isoforms. A panel of cDNAs from different human tissues was used for RT-PCR with the primer pairs specific for the two main isoforms of human *DYRK4* (shown in *A*). Bands detected with the "long" primers correspond to the inclusion/exclusion of exon 6 and/or exon 7, as confirmed by sequencing of the PCR products from the testis. Total DYRK4 expression was assessed with primers from the catalytic domain (*Cat*), and the expression of *GAPDH* was used as a control. *Sk*, skeletal. *D*, conservation of the predicted protein sequence encoded by exon 5 of the *DYRK4* gene. *DYRK4* genes in mammalian genome sequences were identified using the tblastn algorithm at blast.ncbi.nlm.nih.gov. Accession numbers for the genomic sequences are in supplemental Table S3. Basic residues of the putative NLS are shown *underlined in bold*. *Hs, Homo sapiens*; *Pt, Pan troglodytes*; *Mam, Macaca mulatta*; *Rn, Rattus norvegicus*; *Mm, Mus musculus*; *Ec, Equus caballus*; *Bt, Bos taurus*; *Cf, Canis familiaris*; *Md, Monodelphis domestica*; *Oc, Oryctolagus cuniculus*.

sion of an alanine residue in the C-terminal region (supplemental Fig. S2 and supplemental Table S2), probably representing an example of wobble splicing (27). In summary, both human and murine *DYRK4* genes express several transcripts as a result of alternative splicing, with the two main protein products differing in their N-terminal domain.

Differential Expression of Human DYRK4 Variants in Human Tissues—When we analyzed the expression of *DYRK4* in different human tissues by RT-PCR using oligonucleotides matching exons within the catalytic domain, we detected the expression of *DYRK4* mRNA in all the tissues analyzed (Fig. 1*C*). By contrast, *Dyrk4* is predominantly expressed in the testis of the mouse and rat (4, 23). The broader tissue distribution of human DYRK4 is also evident through the sources of the ESTs listed in the Unigene database (www.ncbi.nlm.nih.gov), where 9 of the 10 murine ESTs but only 30 of 150 human ESTs are from testis. Moreover, *DYRK4* mRNA is detected in human cell lines not derived from testis, such as A549 or HEK-293 (supplemental Fig. S4, *A* and *B*), NTERA-2 (28), SH-SY5Y (29), or fibroblasts (30).

PCRs with primer pairs specific for the transcripts encoding the long or the short N-terminal protein variants highlighted the differential expression of the corresponding transcripts, with the long isoform present in several tissues and the short isoform predominantly expressed in testis (Fig. 1*C*). In addition to the bands resulting from the inclusion/exclusion of exon 6, the primers also produced longer PCR products in several tissues. Sequencing of these products showed that they are the result of the inclusion of exon 7 (Fig. 1*C*), which would lead to an in-frame premature stop codon (supplemental Fig. S3*A*). Notably, the ratio between exon 6+/− or 7+/− isoforms was different when distinct tissues were compared (Fig. 1*C*), suggesting that these splicing events are tissue-specific and subjected to regulation.

Alternative Splicing Alters the Subcellular Localization of DYRK4—Human DYRK4 (the 520-amino acid isoform) is located in the cytosol of COS-7 cells when expressed exogenously (23). We confirmed this distribution in HeLa cells using wild-type human DYRK4^{520} and two kinase-deficient mutants (the KR mutant where Lys-133 in the ATP-binding

site is mutated to Arg, and the YF mutant where Tyr-264 in the activation loop is mutated to Phe; see supplemental Fig. S5*A*).

The PSORT II algorithm (31) predicts the presence of a putative bipartite NLS within the extended N-terminal region, which is conserved in the human and murine long protein variants of DYRK4 (Fig. 1*B*). Therefore, we wondered whether the distinct protein isoforms differed in their subcellular distribution. To test this hypothesis, we analyzed the ability of the extended N-terminal region of human and mouse DYRK4 (amino acids 1–100 from hDYRK4^{644}; amino acids 1–64 from mDYRK4^{642}) to translocate a cytosolic protein to the nucleus. We thus generated fusion proteins of the small DYRK4 protein fragments with a chimeric GST-GFP protein, whose size would not allow the proteins to freely diffuse to the nucleus. Whereas GST-GFP was preferentially located in the cytoplasm, the extended DYRK4 N termini drove the accumulation of the chimeric protein in the nucleus, suggesting that active transport is occurring (Fig. 2*A*).

Classic NLSs mediate the nuclear import of proteins through binding to a complex formed by importin α and β1. Importin α is the element within the complex that recognizes the NLSs, both monopartite or bipartite, in the cargo protein (32). To further test the ability of the N terminus of DYRK4 to act as an NLS, we analyzed the binding of this region of the protein to importin α. Thus, lysates of HEK-293T cells expressing the N terminus of hDYRK4^{644} or mDYRK4^{642} fused to GFP were incubated with different bacterially expressed importin α proteins fused to GST, and the protein complexes were recovered with glutathione-Sepharose beads. An interaction with importin α3 and α5 was detected, indicating indeed the presence of a sequence in the DYRK4 N termini able to bind importins (Fig. 2*B*). The lack of binding to importin α1 might reflect the cargo specificity of different importin α isoforms (32). Thus, the localization assay and the importin α pulldown experiments indicated that the first 100/64 amino acids of hDYRK4^{644}/mDYRK4^{642} contain a *bona fide* NLS. In fact, the corresponding full-length human and mouse DYRK4 proteins fused to GFP, which include the putative NLS, were localized to the nucleus of SH-SY5Y cells to a significant extent, whereas GFP-hDYRK4^{520} or GFP-mDYRK4^{594}, which do not have the N-terminal extension, were mainly detected in the cytosol (Fig. 2*C*). However, both isoforms (long and short, in human and mouse) showed similar behavior when overexpressed in HeLa cells (Fig. 2*D*). Together, these results confirm that different DYRK4 isoforms display distinct subcellular localizations, although this might be cell type-dependent. Moreover, these data further suggest that the nuclear accumulation of full-length DYRK4 driven by the NLS is partially prevented by a mechanism that remains to be identified.

For many proteins, their distribution between the cytoplasm and the nucleus is based on a dynamic equilibrium of nuclear import and nuclear export, with contributions from protein retention in any of these subcellular compartments. We reasoned that the preferential cytoplasmic localization of DYRK4 isoforms could result from a strong nuclear export signal-dependent and CRM1 (exportin-1)-mediated nuclear export that might mask the effect of the NLS in the N-terminal extensions of the long DYRK4 isoforms. To determine the contribution of CRM1-mediated nuclear export to the cytosolic accumulation of DYRK4, we exposed cells to the inhibitor of CRM1, leptomycin B. No nuclear accumulation of either isoform was evident after 4 h in the presence of this inhibitor (Fig. 3*A*).

The DYRK4 isoforms showed a preferential cytoplasmic localization; however, low amounts of the proteins were also detectable in the nucleus by confocal microscopy (clearly visible after the cytoplasm was bleached; see Fig. 3*B* and supplemental Fig. S5*C*). To answer the question whether the observed subcellular distribution is based on a dynamic equilibrium of constant nuclear export and nuclear import, we analyzed the dynamics of DYRK4 shuttling in single living cells using the FLIP technique (33). A defined ROI in the cytoplasm was subjected to repeated photobleaching to wipe out the cytoplasmic GFP fluorescence (Fig. 3*B*, *time point 0*). Subsequent reduction in GFP fluorescence in the nucleus reflects the nucleocytoplasmic shuttling of bleached protein into the nucleus and nonbleached protein out of the nucleus. The diffusible character of unfused GFP was reflected in its fast nucleocytoplasmic shuttling, which reached equilibrium after 7 min (Fig. 3, *B* and *C,* and supplemental Fig. S5, *C* and *D*). The two isoforms of mDYRK4 displayed distinct nucleocytoplasmic shuttling, with the nucleocytoplasmic exchange of the shorter isoform (mDYRK4^{594}) converging to equilibrium and shuttling more slowly (see graph in Fig. 3*C*, *middle panel,* and supplemental videos 1 and 2). Treatment with leptomycin B had no effect on mDYRK4^{594} nucleocytoplasmic shuttling, further supporting that nuclear export was independent of CRM1 (supplemental Fig. S5*B*). By contrast, cytoplasmic bleaching of the longer isoform (mDYRK4^{642}) did not significantly decrease GFP fluorescence in the nucleus, indicating that this isoform did not exit the nucleus. Similar results were obtained when the corresponding human isoforms (hDYRK4^{520} and hDYRK4^{644}) were assayed (supplemental Fig. S5, *C* and *D*). The static nature of the long DYRK4 isoform could indicate that it is retained in the nucleus by strong interactions with nuclear proteins or chromatin. Taken together, these results indicate that the alternatively spliced N-terminal region, common to human and mouse, confers distinct cellular properties to DYRK4.

Autophosphorylation of DYRK4 in the Activation Loop Is Required for Kinase Activity—All members of the DYRK family studied so far are autophosphorylated at a conserved tyrosine motif in the activation loop (Y*X*Y), within the catalytic domain (10). Indeed, phosphorylation of the second tyrosine residue is required for the complete activation of DYRK protein kinases (11, 34). To test whether this is also the case for DYRK4, we generated a mutant version of human DYRK4^{520} in which the second tyrosine of the Y*X*Y motif (Tyr-264) was mutated to phenylalanine (DYRK4^{YF}). Although immunoblotting of DYRK4 overexpressed in HEK-293 cells revealed that DYRK4 is indeed tyrosine-phosphorylated (Fig. 4*A*), in neither the kinase-deficient mutant DYRK4^{KR} nor the DYRK4^{YF} mutant were phosphotyrosines detected with a phosphotyrosine-specific antibody (Fig. 4*A*). Mass spectrometry analysis confirmed that Tyr-264 in the activation loop was phosphor-

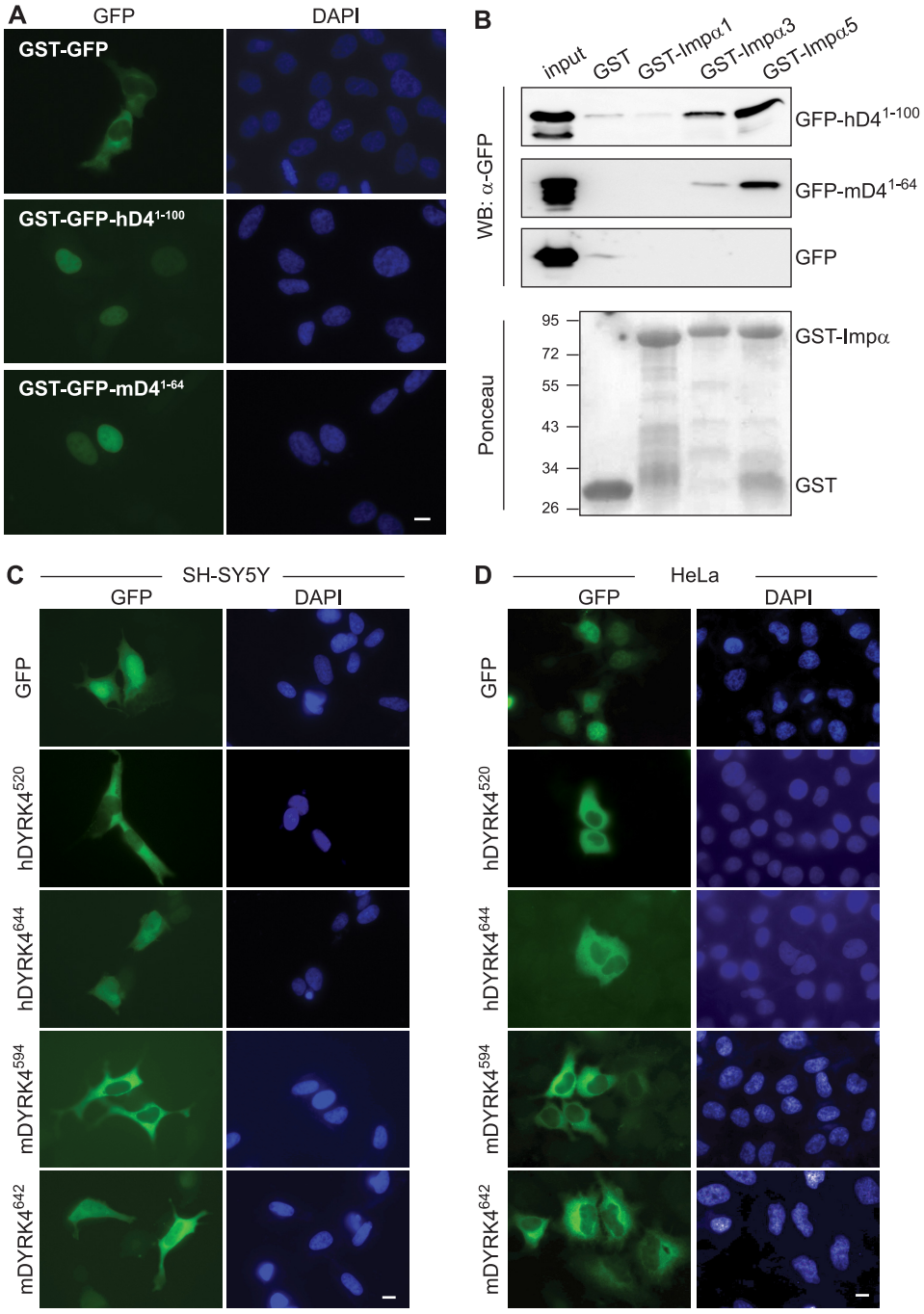

FIGURE 2. **Characterization of the putative NLS in DYRK4.** *A*, functional NLS in the N-terminal region of DYRK4. The chimeric GST-GFP protein, or a fusion of the first 100 amino acids of hDYRK4^{644} or the first 64 amino acids of mDYRK4^{642} to this protein, was expressed in HeLa cells, and the subcellular localization was analyzed by fluorescence microscopy. Representative images are shown. *B*, pulldown analysis of GST-importin-α1, -α3, and -α5 fusion proteins expressed and purified from bacteria, and soluble lysates of cells expressing unfused GFP, GFP fused to the N-terminal region of hDYRK4 (1–100 amino acids), or mDYRK4 (1–64 amino acids). Bound proteins were analyzed in Western blot (*WB*) with anti-GFP. Unfused GST was used as a negative control for binding. Membranes were stained with Ponceau S Red to show loading of GST-importin-α fusions. *C* and *D*, unfused GFP or GFP fused to hDYRK4^{520}, hDYRK4^{644}, mDYRK4^{594}, and mDYRK4^{642} were expressed in SH-SY5Y (*C*) or HeLa (*D*) cells, and their subcellular localization was analyzed by fluorescence microscopy. *A*, *C*, and *D*, the nuclei were stained with DAPI. *Scale bars,* 10 μm.

ylated (Fig. 4*B*), yet no differences in tyrosine phosphorylation were evident when the long and the short human DYRK4 isoforms were compared (Fig. 4*C*). Moreover, the DYRK4^{YF} mutant was neither autophosphorylated nor displayed kinase activity on a synthetic substrate, the exogenous peptide substrate DYRKtide (designed on the basis of the phosphorylation consensus sequence for DYRK1A (Fig. 4, *D* and *E*) (12). Together, these results show that DYRK4 is autophosphorylated on tyrosine residues and that the phosphorylation of the second tyrosine in the YXY motif is necessary for its kinase activity.

DYRK4 expressed in mammalian cells migrates as a doublet in SDS gels (Fig. 4*A*). The appearance of the low electrophoretic mobility band does not depend on autophosphoryla-

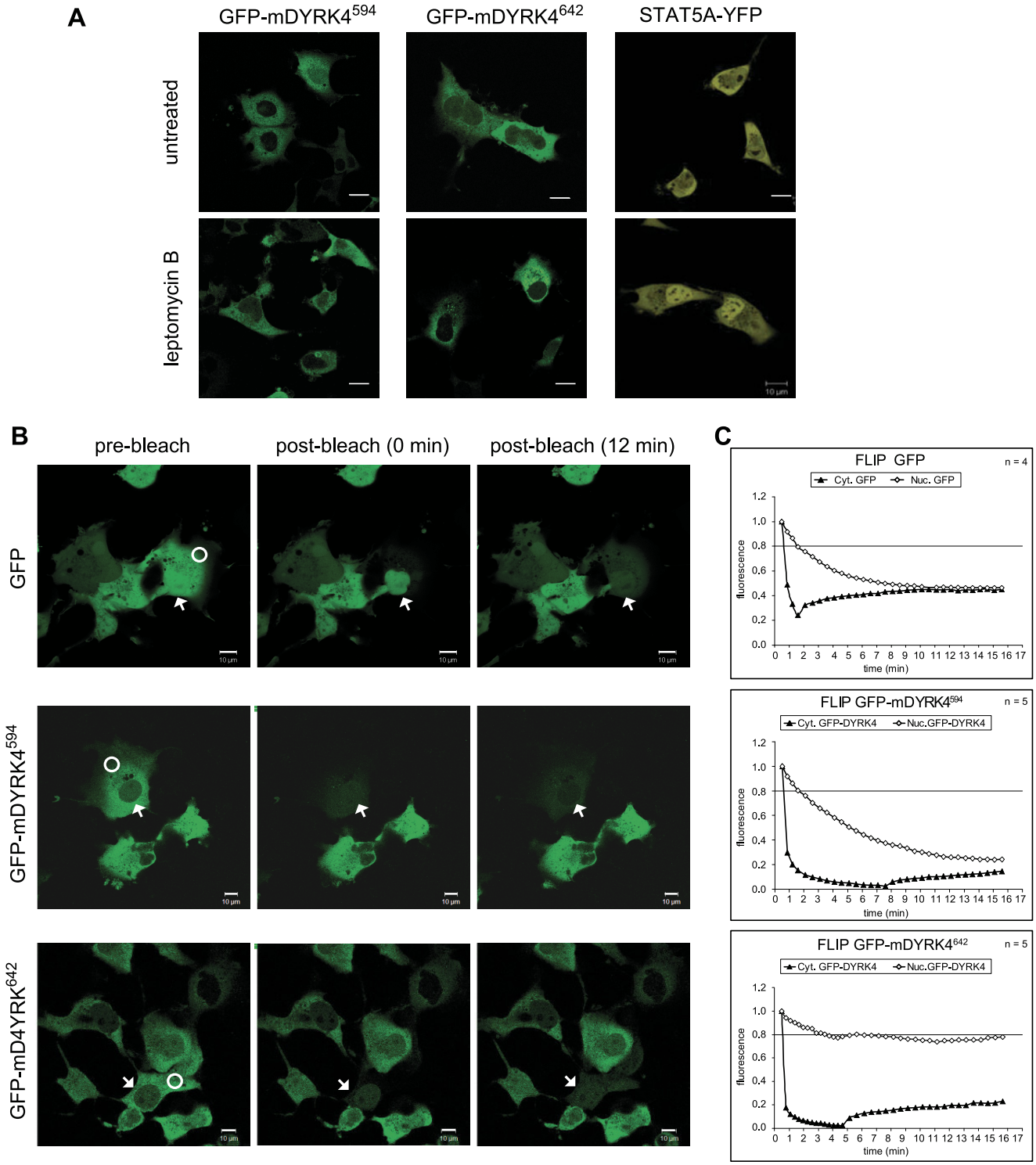

FIGURE 3. **Nucleocytoplasmic distribution of DYRK4.** *A*, CRM1-independent distribution of GFP-mDYRK4. The subcellular localization of GFP-mDYRK4^{594} and GFP-mDYRK4^{642} expressed in COS-7 cells was analyzed before (untreated) and 4 h after addition of leptomycin B. STAT5A fused to YFP was used as a positive control responding to CRM1 inhibition. *B*, differences in nucleocytoplasmic shuttling of GFP-DYRK4 isoforms. Cytoplasmic FLIP analysis was performed on GFP, GFP-mDYRK4^{594}, or GFP-mDYRK4^{642} expressed in COS-7 cells. The *panels* show representative images in which the bleached area is indicated with a *white circle* and the nucleus with an *arrow*. *C*, fluorescence was measured in the cytoplasmic and nuclear regions of interest along the time period represented. The diagrams show the averaged normalized fluorescence intensities of $n = 4$ or 5 experiments as indicated. *Scale bars*, 10 μm.

tion, because the band is also present in the two kinase-deficient mutants (Fig. 4, *A*, *D*, and *F*). Nevertheless, treatment of DYRK4 proteins with phosphatase led to the disappearance of the slower migrating band (Fig. 4*F*). Mass spectrometry analysis of hDYRK4^{520} expressed in mammalian cells, both the wild-type and a kinase-inactive version, identified several peptides with phosphorylated residues (supplemental Fig. S6), indicating that DYRK4 is phosphorylated by cellular kinases.

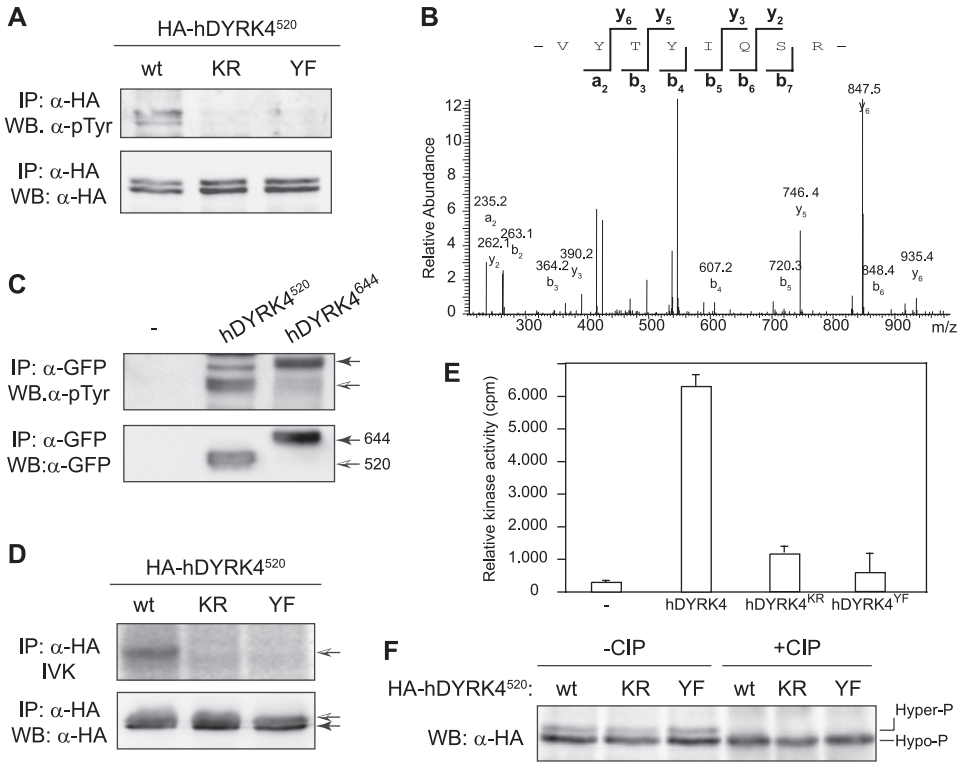

FIGURE 4. **Phosphorylation of the *YXY* motif is required for DYRK4 kinase activity.** *A*, DYRK4 is tyrosine-phosphorylated. Extracts of HEK-293 cells expressing HA-hDYRK4^{520} WT, KR, or YF mutants were immunoprecipitated (*IP*) with an anti-HA antibody and analyzed in Western blot (*WB*) with anti-HA and anti-phosphotyrosine antibodies as indicated. *B*, MS/MS spectrum of the phosphopeptide VYTY(P)IQSR from wild-type HA-hDYRK4^{520}. *C*, human DYRK4^{520} and DYRK4^{644} fused to GFP were analyzed by Western blot with anti-phosphotyrosine and anti-GFP antibodies. *D* and *E*, phosphorylation of the *YXY* motif is required for DYRK4 kinase activity. Cell extracts expressing HA-hDYRK4^{520} WT or the mutant HA-hDYRK4^{KR} or HA-hDYRK4^{YF} versions were immunoprecipitated with anti-HA and the immunocomplexes were subjected to an IVK assay using DYRKtide as the exogenous substrate (*E*). DYRK4 autophosphorylation was assessed by autoradiography of dried gels (*D*). The bands corresponding to DYRK4 are indicated with *arrows*. The *graph* in *E* represents the means ± S.D. of two independent experiments performed in triplicate. Equal protein loading was confirmed by anti-HA probing of Western blots. *F*, DYRK4 is phosphorylated by cellular kinases. Immunoprecipitates of HA-hDYRK4^{520} or its kinase-deficient derivatives were split in several aliquots that were incubated in the absence or presence of calf intestinal phosphatase (*CIP*). The hyper- and hypophosphorylated forms are indicated.

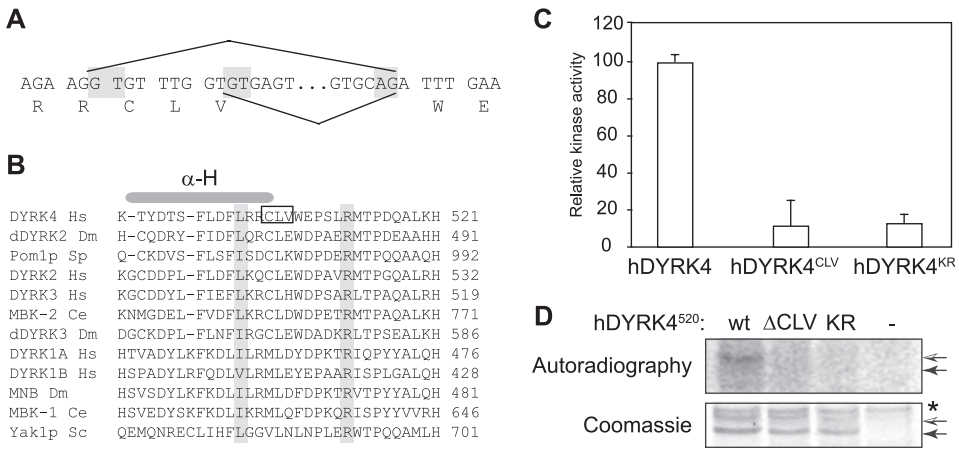

FIGURE 5. **Alternative splicing affects the catalytic properties of DYRK4.** *A*, alternative splicing affecting exon 19. Acceptor and donor sites are highlighted in *gray*. *B*, amino acid comparison of the kinase subdomain XI of several DYRK family members, including α-helix H (*α-H*). The accession numbers are provided in the supplemental Table S3. The invariant arginine residue in this subdomain and the highly conserved leucine are highlighted in *gray*. The CLV deletion in DYRK4 is indicated. *C* and *D*, cell extracts expressing HA-hDYRK4^{520} or the corresponding mutants HA-hDYRK4^{KR} or HA-hDYRK4$^{\Delta CLV}$ were immunoprecipitated with anti-HA, and the immunocomplexes were subjected to an IVK assay using DYRKtide (*C*). The *graph* represents the means ± S.D. of three independent experiments performed in triplicate (relative activity as percentage of DYRK4 wild type). DYRK4 autophosphorylation was assessed by autoradiography of dried gels (*D*). Equal amount of protein in the immunoprecipitated samples was confirmed by Coomassie staining of the gels, and the bands corresponding to DYRK4 are indicated with *arrows*. The *asterisk* shows a nonspecific band.

Use of an Alternative Splicing Donor Site in Exon 19 Alters DYRK4 Activity—The alternative use of different 5′-exons does not affect the catalytic domain of DYRK4, and accordingly both the long and short isoforms are catalytically active protein kinases (supplemental Fig. S7*A*). In contrast, we found differences in the kinase activity of variants derived from an-

other splicing event affecting both human and mouse DYRK4 that involved the use of an alternative splicing donor site in exon 19 (Fig. 5*A*). This event leads to the deletion/inclusion of three amino acids, CLV, at the end of the α-helix H, immediately prior to the conserved arginine residue in subdomain XI of the kinase domain (Fig. 5*B*). To assess the impact of this small deletion on DYRK4 enzymatic activity, we compared the *in vitro* behavior of hDYRK4^{520} wild type and the corresponding mutant hDYRK4$^{\Delta CLV}$ in kinase assays. The autophosphorylation activity of the CLV-deleted protein was greatly impaired, as was its ability to phosphorylate an exogenous peptide (Fig. 5, *C* and *D*). The central leucine residue within the CLV triplet corresponds to one of the α-helix H hydrophobic residues involved in anchoring to α-helix F (35). The interaction between these two helices is thought to play an important role in forming the substrate-binding structure (35), and altering this interaction may induce changes in catalytic activity. Therefore, our results indicate that an alternative splicing event influences the catalytic properties of the resulting DYRK4 protein isoform.

Substrate Specificity of DYRK4—When characterizing the catalytic activity of DYRK4, we found that the phosphorylation of DYRKtide by DYRK4 was much less efficient than that by DYRK1A (supplemental Fig. S7, *B–D*). Hence, DYRKtide may not be an optimal substrate for DYRK4, and thus, we examined whether DYRK4 exhibited different substrate specificity than other members of the DYRK family. Accordingly, the phosphorylation specificity of DYRK4, or representative mammalian class I and class II DYRKs (DYRK1A and DYRK2, respectively), was studied in phosphosite arrays containing 720 peptides derived from annotated phosphorylation sites in human proteins (Fig. 6*A*). Reassuringly, two known phosphorylation sites of DYRK1A, Thr-212 in Tau and Ser-640 in glycogen synthase (13, 14), were considered to be among the best peptide substrates of DYRK1A in these arrays (supplemental Table S4). In a test for reproducibility, classification of 27 out of 720 peptides differed between two independent experiments with different batches of arrays, whereas only 9 of 720 peptides were differently classified in parallel reactions with arrays from the same batch (supplemental Fig. S8, *A* and *B*). The experiment presented in Fig. 6 was done with arrays from the same batch.

An analysis of the top 30 peptide substrates for DYRK4 revealed that 24 contained a serine or threonine residue followed by a proline (Fig. 6*B* and supplemental Table S4), indicating that DYRK4, like DYRK1A, can be classified as a proline-directed kinase (12). However, the requirement for the proline appeared to be less stringent for DYRK4 than for DYRK1A. An arginine residue at position P −3 or P −2 was previously shown to be important for optimal substrate recognition by DYRK1A and DYRK2 (12, 15). Arginines at P −2 or P −3 were present in 17 of the 30 best substrates of DYRK1A but were much less represented in the DYRK4 and DYRK2 datasets (7 or 9 out of 30; Fig. 6*B* and supplemental Table S4). Interestingly, only one-third of the peptides phosphorylated by DYRK4 were also substrates of DYRK1A or DYRK2 (50% of the top 30; Fig. 6*C*). Moreover, 10 peptides were phosphorylated by both DYRK4 and DYRK2 but not by DYRK1A,

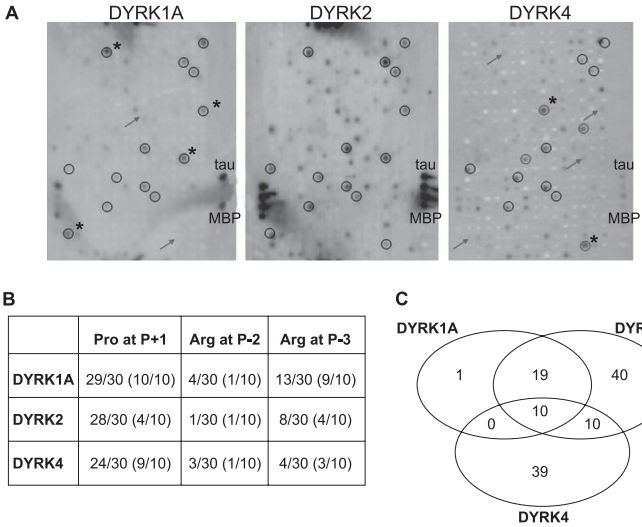

	Pro at P+1	Arg at P-2	Arg at P-3
DYRK1A	29/30 (10/10)	4/30 (1/10)	13/30 (9/10)
DYRK2	28/30 (4/10)	1/30 (1/10)	8/30 (4/10)
DYRK4	24/30 (9/10)	3/30 (1/10)	4/30 (3/10)

FIGURE 6. **Identification of specific substrates for DYRK4.** *A*, specificity of DYRK4 (hDYRK4^{520}), DYRK1A$^{\Delta C}$, and DYRK2 was determined using a phosphorylation of peptide arrays as indicated under "Experimental Procedures." Only a section of the array is shown. Peptides phosphorylated by all three kinases are *circled*. Peptides positive for either DYRK1A or DYRK4 (*asterisks*) but not for the other (*arrows*) are marked. Only peptides exceeding a threshold intensity of 20% of the strongest signal on the array were considered positive. Four spots contained control proteins (including Tau and myelin basic protein (*MBP*)) to define the position of the array on the autoradiograph. *B*, congruence of the peptide substrates identified on the phosphosite array with the consensus target sequence for DYRK1A. The occurrence of the amino acids matching the DYRK1A consensus target site (Rx$_{1-2}$(S/T)P) in the top 30 and the top 10 substrates (in *parentheses*) of DYRK1A, DYRK2, and DYRK4 is listed. Several peptides harbor more than one possible phosphorylation site, and one peptide (Pep269) contains arginines at both P −2 and P −3 (see supplemental Table S4). *C*, distribution of the peptides phosphorylated exclusively by only one DYRK or by two or all three DYRKs are shown in the Venn diagram.

whereas no substrate was recognized by DYRK4 and DYRK1A but not by DYRK2 (Fig. 6*C*).

To confirm that the substrate specificity of DYRK4 differed from that of DYRK1A, we selected a peptide specifically recognized by DYRK4 for further analysis. Peptide 285 mimics Ser-73 in c-Jun (Fig. 7*A*), and it was chosen as the top scoring DYRK4 substrate whose phosphorylation by DYRK1A or DYRK2 was sub-threshold (supplemental Table S4). For comparison, DYRKtide was used as nonspecific peptide substrate for all kinases of the DYRK family (12). Phosphorylation assays confirmed that Pep285 was phosphorylated by DYRK4 but not by DYRK1A and DYRK2 (Fig. 7*B*), supporting the proposal that DYRK4 can phosphorylate target sequences not recognized by DYRK1A or DYRK2. These experiments were performed with recombinant kinases expressed in *E. coli* (DYRK1A and DYRK2) or in insect cells (DYRK4), and thus, we also assayed the activity of DYRK4 and DYRK1A isolated from HeLa cells on Pep285 and two other DYRK substrates, Pep3 and SAPtide (Fig. 7*A*). These assays showed that Pep285 was the only peptide phosphorylated distinctly by DYRK1A and DYRK4 (Fig. 7*C* and supplemental Fig. S8*C*).

DISCUSSION

The DYRK family of protein kinases is composed of five members in mammals, of which DYRK1A, DYRK1B, DYRK2, and DYRK3 have been studied extensively due to their roles in cell differentiation and survival and their critical participation

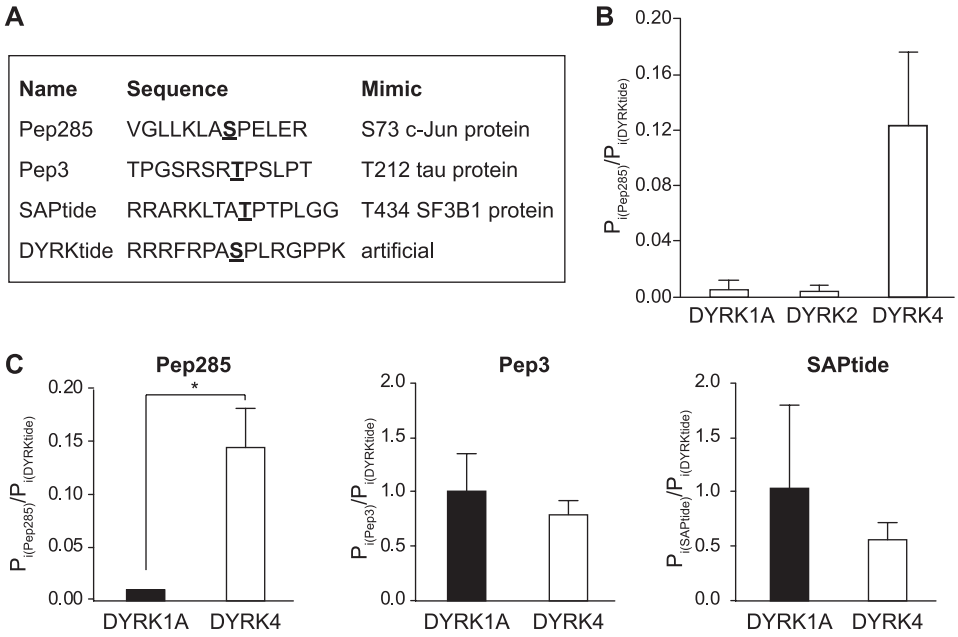

FIGURE 7. **Differential DYRK4 peptide phosphorylation.** *A*, amino acid sequence of the peptides used in this study. *B*, Pep285 is a specific substrate for DYRK4. Peptide phosphorylation by bacterially expressed GST-DYRK1A$^{\Delta C}$ or GST-DYRK2, and commercial GST-DYRK4 (hDYRK4^{520}) expressed in Sf9 cells, was measured as the extent of phosphate incorporated into DYRKtide and Pep285. The *histogram* represents the ratio of Pep285 phosphorylation to DYRKtide phosphorylation by the indicated kinases after 30 min of the IVK reaction (means ± S.D. from three experiments). *C*, peptide selectivity of DYRK4. Anti-GFP immunocomplexes from HeLa cells expressing GFP-DYRK1A or GFP-hDYRK4^{520} were assessed in an IVK assay with different peptides as the substrates. Incorporation of ^{33}P into the indicated peptides was normalized to the phosphate incorporation into DYRKtide. The *histogram* represents the means ± S.D. from three independent experiments (*, $p = 0.0232$; paired *t* test). Raw data corresponding to these experiments is shown in supplemental Fig. S8*C*.

in processes such as neurogenesis or cancer (2). By contrast, very little is known about the fifth member of the family, DYRK4. Our characterization of mammalian DYRK4 highlights several aspects that are common to DYRKs, such as the mode of activation or the subcellular distribution as a regulatory mechanism. However, other features such as substrate specificity were also characterized that could be important for establishing functional differences between DYRK family members.

DYRK4 Gene Expression and Regulation by Alternative Splicing—Several distinct transcripts of human and mouse *DYRK4* are expressed, each encoding distinct protein products, due to alternative promoter use and first exon choice, as evident for other mammalian *DYRK* genes (2). By contrast to the restricted expression in the testis of rodents (4, 23), human *DYRK4* shows a broad pattern of expression in various tissues that is suggestive of a functional divergence between mouse and humans, and which severely limits the value of mouse models for the functional analysis of human DYRK4. The proposal that DYRK4 has acquired different functions during evolution is also supported by the unusually weak sequence conservation between human and mouse DYRK4 when compared with other orthologous DYRK pairs (Fig. 8).

The existence of distinct promoters probably underlies the differential expression pattern of the two *DYRK4* 5′ variants in human tissues. Surprisingly, the transcript for the short N-terminal DYRK4 isoform appears to be limited to the testis in humans, although the corresponding 5′-exon is not conserved in the mouse. Further variants are generated by distinct alternative splicing events, some of which lead to small in-frame deletions/insertions, whereas others give rise to aberrant protein products. In particular, the exclusion of exon 18 is a frequent event, documented in about one-third of the ESTs in the data base (supplemental Table S2), and it would give rise to a truncated protein that lacks the C-terminal end of the kinase domain and that is therefore predicted to be catalytically inactive. This situation resembles the splicing of DYRK1B that affects a region between subdomains X and XI and that renders a kinase-deficient isoform (36). Kinase-independent activities of several DYRK proteins have already been reported, suggestive of a scaffolding role for these proteins rather than a catalytic one (37–40). Hence, we cannot rule out that DYRK4 proteins lacking catalytic activity, such as the truncated protein resulting from exon 18 skipping or the small CLV deletion affecting α-helix H, may be biologically active.

Subcellular Localization of DYRK4 Could Represent a Regulatory Mechanism—The subcellular localization of proteins larger than 45 kDa (the exclusion size of the nuclear pore), such as DYRK4, depends on several mechanisms, including active nuclear import, active nuclear export, and nuclear or cytosolic retention. Our results show that all these mechanisms could act on DYRK4, and they might indeed contribute to the regulation of the biological activity of DYRK4 by altering the possibility of finding substrates or modulators in particular subcellular compartments.

The short isoform of human DYRK4 was characterized, and GFP-DYRK4^{520} was localized in the cytosol of COS-7 cells (23). We demonstrate that the newly identified long DYRK4 isoform (both in human and mouse) has a different subcellular localization and that the extended N-terminal region, which is highly conserved, accounts for this difference

A

		C. elegans		*D. melanogaster*		
		MBK-1	MBK-2	MNB	dDYRK2	dDYRK3
H. sapiens	DYRK1A	80%	61%	91%	62%	59%
	DYRK1B	73%	59%	87%	58%	59%
	DYRK2	58%	85%	61%	71%	85%
	DYRK3	58%	80%	59%	67%	80%
	DYRK4	56%	71%	61%	74%	69%

B

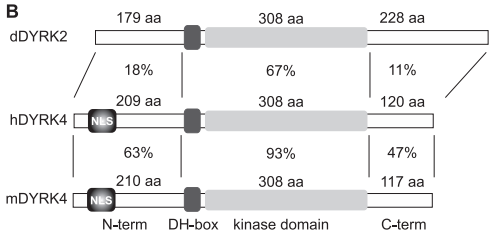

FIGURE 8. **Homology within the DYRK family members.** *A*, comparison of the members of the DYRK family from different species. The amino acid (*aa*) identity calculated by BLAST (blastp) is given as percentage. *B*, detailed comparison of the noncatalytic N-terminal (*N-term*) and C-terminal (*C-term*) and kinase domain (including the DH-box) in human DYRK4 with those of *Drosophila* dDYRK2 and murine DYRK4 as the closest homologues. Sequence sources are listed in the supplemental Table S3.

(Fig. 8*B*). The N-terminal extension harbors a classic NLS based on the positive binding to importin α and on the nuclear import of a heterologous protein when fused to it. In addition, the extended N-terminal region mediates the nuclear retention of the long isoform (hDYRK4^{644} or mDYRK4^{642}), as suggested by the lack of nucleocytoplasmic shuttling in FLIP experiments. Given that detectable amounts of hDYRK4^{520} and mDYRK4^{594}, which lack the conserved N-terminal NLS, could be detected in the nucleus, it is possible that a second NLS could exist in DYRK4, such as that described between the kinase subdomains X and XI in DYRK1A (41).

DYRK4 long isoform was only partially segregated in the nucleus suggesting that full nuclear accumulation was prevented by mechanisms such as strong CRM1-independent nuclear export, NLS masking, or an interaction with cytosolic proteins. Nuclear translocation in response to extracellular cues has been demonstrated for DYRK2 or yeast Yak1p (16, 19), which could be a common feature of this family of kinases. Further research should help uncover the signals that modulate the subcellular localization of DYRK4. Finally, given that NLSs have been identified in DYRK4 (this study) and DYRK2 (19) and that DYRK3 is also at least partially localized in the nucleus (22, 42), the distinction of "cytosolic" class II DYRKs from the "nuclear" class I DYRKs must be regarded as an oversimplification of the complex behavior of these kinases.

DYRK4 Catalytic Activity and Substrate Specificity—Like other DYRKs (9, 43–45), our mutational analysis indicates that phosphorylation of the second tyrosine residue within the activation loop (the *YXY* motif) appears to be necessary for the full activity of DYRK4. The fact that bacterially expressed GST-DYRK4 was catalytically active and that the MS analysis found that wild type, but not a kinase-deficient mutant of DYRK4, was phosphorylated in the second tyrosine of the activation loop is an indication that DYRK4 autophosphorylates the activation loop tyrosine. These findings fit with the current model for the activation of DYRKs (11), although it remains to be established whether DYRK4 behaves as a *bona fide* class II DYRK in terms of the contribution of the NAPA domain to the activation process (7). The inhibitory effect of manganese cations on the activity of class II *Drosophila* dDYRK2 (the fly orthologue of DYRK4; Fig. 8*A*) is noteworthy (9), as also observed in human DYRK4 (supplemental Fig. S7*D*), suggesting that the evolutionary relationship is translated into functional features.

We identify phosphorylated residues outside the catalytic domain in both wild type and a kinase-inactive DYRK4, which indicates that DYRK4 is phosphorylated by upstream kinases. Hence, DYRK4 could be modulated by phosphorylation, although we still do not know the processes that are affected by such regulation. Regulatory phosphorylation of other DYRKs has been reported recently, as in the case of MBK-2 by casein kinase I or DYRK2 by MAP3K2 and ataxia telangiectasia mutated kinase (17, 46, 47).

The substrate specificity of DYRKs has been little explored, although DYRK1A, DYRK2, and DYRK3 have previously been reported to differ in their specificities toward protein and peptide substrate (4, 15). However, only a few substrates were compared in these studies because the experiments were directed toward systematically analyzing the importance of specific residues in a given peptide on substrate recognition (4, 15). The experimental setup employed here offers a broader view by using an array with peptides that reflect known human phosphorylation sites. The validity of the assay was not only supported by the identification of two known DYRK1A phosphorylation sites but also by the fact that the majority of the peptides phosphorylated by DYRK1A match its consensus target sequence, with a proline at P +1 and an arginine at P −3 (12). However, the relatively high number of DYRK substrates that do not contain an arginine residue at P −3 or P −2 contrasts with the almost absolute requirement for the arginine observed elsewhere (15), where DYRKs were considered as arginine-directed protein kinases. This difference is most likely due to the fact that in the previous study the importance of the arginine was only tested in the context of one specific DYRK target site (Ser-539 in eIF2Bϵ), whereas the phosphosite array contains a large selection of diverse peptides. One example of an arginine-independent target site of DYRK1A is Thr-434 in SF3B1 (48), which is mimicked by the peptide SAPtide, a peptide that is phosphorylated with a similar efficiency as DYRKtide by both DYRK1A and DYRK4.

We found that DYRK1A, DYRK2, and DYRK4 phosphorylate distinct although overlapping sets of the 720 different peptides in the phosphosite array. These results lead to the conclusion that DYRK2 and DYRK4 are much less biased toward peptides with an arginine in the P −2 or P −3 position than DYRK1A, which is consistent with the identification of DYRK2 as a p53 kinase targeting Ser-46 within the DDLML-**S**PDDI motif (19). The fact that DYRK4 shares several peptide substrates with DYRK2 that are not phosphorylated by DYRK1A may reflect the closer evolutionary relationship be-

tween these class II DYRKs. Moreover, and based on the results of the phosphosite array, we have identified a peptide (Pep285) that could be used as a specific substrate for DYRK4 in kinase assays.

As a final consideration, and given that human DYRKs appear to be co-expressed in different tissues and that they could be localized in the same subcellular compartments, substrate specificity may represent a critical factor that governs biological specificity among this family of protein kinases. Further research will be necessary to positively identify the structural determinants that distinguish target site recognition by DYRK4 from that of the other members of the DYRK family.

Acknowledgments—We wholeheartedly appreciate the technical assistance of A. Raya, and we thank M. Sefton for English editorial work. The MS-based phosphopeptide analysis was carried out in the Joint UPF/CRG Proteomics Facility at Parc de Recerca Biomèdica de Barcelona, a member of ProteoRed network. We also thank C. Chiva and H. Molina for their assistance.

REFERENCES

1. Park, J., Song, W. J., and Chung, K. C. (2009) *Cell. Mol. Life Sci.* **66,** 3235–3240
2. Aranda, S., Laguna, A., and de la Luna, S. (2011) *FASEB J.,* in press
3. Becker, W., and Joost, H. G. (1999) *Prog. Nucleic Acids Res. Mol. Biol.* **62,** 1–17
4. Becker, W., Weber, Y., Wetzel, K., Eirmbter, K., Tejedor, F. J., and Joost, H. G. (1998) *J. Biol. Chem.* **273,** 25893–25902
5. Raich, W. B., Moorman, C., Lacefield, C. O., Lehrer, J., Bartsch, D., Plasterk, R. H., Kandel, E. R., and Hobert, O. (2003) *Genetics* **163,** 571–580
6. Tejedor, F., Zhu, X. R., Kaltenbach, E., Ackermann, A., Baumann, A., Canal, I., Heisenberg, M., Fischbach, K. F., and Pongs, O. (1995) *Neuron* **14,** 287–301
7. Kinstrie, R., Luebbering, N., Miranda-Saavedra, D., Sibbet, G., Han, J., Lochhead, P. A., and Cleghon, V. (2010) *Sci. Signal.* **3,** ra16
8. Bähler, J., and Pringle, J. R. (1998) *Genes Dev.* **12,** 1356–1370
9. Lochhead, P. A., Sibbet, G., Kinstrie, R., Cleghon, T., Rylatt, M., Morrison, D. K., and Cleghon, V. (2003) *Biochem. J.* **374,** 381–391
10. Becker, W., and Sippl, W. (2011) *FEBS J.* **278,** 246–256
11. Lochhead, P. A., Sibbet, G., Morrice, N., and Cleghon, V. (2005) *Cell* **121,** 925–936
12. Himpel, S., Tegge, W., Frank, R., Leder, S., Joost, H. G., and Becker, W. (2000) *J. Biol. Chem.* **275,** 2431–2438
13. Skurat, A. V., and Dietrich, A. D. (2004) *J. Biol. Chem.* **279,** 2490–2498
14. Woods, Y. L., Cohen, P., Becker, W., Jakes, R., Goedert, M., Wang, X., and Proud, C. G. (2001) *Biochem. J.* **355,** 609–615
15. Campbell, L. E., and Proud, C. G. (2002) *FEBS Lett.* **510,** 31–36
16. Moriya, H., Shimizu-Yoshida, Y., Omori, A., Iwashita, S., Katoh, M., and Sakai, A. (2001) *Genes Dev.* **15,** 1217–1228
17. Cheng, K. C., Klancer, R., Singson, A., and Seydoux, G. (2009) *Cell* **139,** 560–572
18. Mercer, S. E., Ewton, D. Z., Shah, S., Naqvi, A., and Friedman, E. (2006) *Cancer Res.* **66,** 5143–5150
19. Taira, N., Nihira, K., Yamaguchi, T., Miki, Y., and Yoshida, K. (2007) *Mol. Cell* **25,** 725–738
20. Zhang, D., Li, K., Erickson-Miller, C. L., Weiss, M., and Wojchowski, D. M. (2005) *Genomics* **85,** 117–130
21. Geiger, J. N., Knudsen, G. T., Panek, L., Pandit, A. K., Yoder, M. D., Lord, K. A., Creasy, C. L., Burns, B. M., Gaines, P., Dillon, S. B., and Wojchowski, D. M. (2001) *Blood* **97,** 901–910
22. Lord, K. A., Creasy, C. L., King, A. G., King, C., Burns, B. M., Lee, J. C., and Dillon, S. B. (2000) *Blood* **95,** 2838–2846
23. Sacher, F., Möller, C., Bone, W., Gottwald, U., and Fritsch, M. (2007) *Mol. Cell. Endocrinol.* **267,** 80–88
24. Alvarez, M., Altafaj, X., Aranda, S., and de la Luna, S. (2007) *Mol. Biol. Cell* **18,** 1167–1178
25. de Graaf, K., Hekerman, P., Spelten, O., Herrmann, A., Packman, L. C., Büssow, K., Müller-Newen, G., and Becker, W. (2004) *J. Biol. Chem.* **279,** 4612–4624
26. Schutkowski, M., Reimer, U., Panse, S., Dong, L., Lizcano, J. M., Alessi, D. R., and Schneider-Mergener, J. (2004) *Angew. Chem. Int. Ed. Engl.* **43,** 2671–2674
27. Hiller, M., and Platzer, M. (2008) *Trends Genet.* **24,** 246–255
28. Leypoldt, F., Lewerenz, J., and Methner, A. (2001) *J. Neurochem.* **76,** 806–814
29. Reimertz, C., Kögel, D., Rami, A., Chittenden, T., and Prehn, J. H. (2003) *J. Cell Biol.* **162,** 587–597
30. Kyng, K. J., May, A., Kølvraa, S., and Bohr, V. A. (2003) *Proc. Natl. Acad. Sci. U.S.A.* **100,** 12259–12264
31. Nakai, K., and Horton, P. (2007) *Methods Mol. Biol.* **390,** 429–466
32. Lange, A., Mills, R. E., Lange, C. J., Stewart, M., Devine, S. E., and Corbett, A. H. (2007) *J. Biol. Chem.* **282,** 5101–5105
33. Lippincott-Schwartz, J., Snapp, E., and Kenworthy, A. (2001) *Nat. Rev. Mol. Cell Biol.* **2,** 444–456
34. Himpel, S., Panzer, P., Eirmbter, K., Czajkowska, H., Sayed, M., Packman, L. C., Blundell, T., Kentrup, H., Grötzinger, J., Joost, H. G., and Becker, W. (2001) *Biochem. J.* **359,** 497–505
35. Kornev, A. P., Taylor, S. S., and Ten Eyck, L. F. (2008) *Proc. Natl. Acad. Sci. U.S.A.* **105,** 14377–14382
36. Leder, S., Czajkowska, H., Maenz, B., De Graaf, K., Barthel, A., Joost, H. G., and Becker, W. (2003) *Biochem. J.* **372,** 881–888
37. von Groote-Bidlingmaier, F., Schmoll, D., Orth, H. M., Joost, H. G., Becker, W., and Barthel, A. (2003) *Biochem. Biophys. Res. Commun.* **300,** 764–769
38. Sitz, J. H., Tigges, M., Baumgärtel, K., Khaspekov, L. G., and Lutz, B. (2004) *Mol. Cell. Biol.* **24,** 5821–5834
39. Kelly, P. A., and Rahmani, Z. (2005) *Mol. Biol. Cell* **16,** 3562–3573
40. Maddika, S., and Chen, J. (2009) *Nat. Cell Biol.* **11,** 409–419
41. Alvarez, M., Estivill, X., and de la Luna, S. (2003) *J. Cell Sci.* **116,** 3099–3107
42. Guo, X., Williams, J. G., Schug, T. T., and Li, X. (2010) *J. Biol. Chem.* **285,** 13223–13232
43. Kentrup, H., Becker, W., Heukelbach, J., Wilmes, A., Schürmann, A., Huppertz, C., Kainulainen, H., and Joost, H. G. (1996) *J. Biol. Chem.* **271,** 3488–3495
44. Kassis, S., Melhuish, T., Annan, R. S., Chen, S. L., Lee, J. C., Livi, G. P., and Creasy, C. L. (2000) *Biochem. J.* **348,** 263–272
45. Lee, K., Deng, X., and Friedman, E. (2000) *Cancer Res.* **60,** 3631–3637
46. Varjosalo, M., Björklund, M., Cheng, F., Syvänen, H., Kivioja, T., Kilpinen, S., Sun, Z., Kallioniemi, O., Stunnenberg, H. G., He, W. W., Ojala, P., and Taipale, J. (2008) *Cell* **133,** 537–548
47. Taira, N., Yamamoto, H., Yamaguchi, T., Miki, Y., and Yoshida, K. (2010) *J. Biol. Chem.* **285,** 4909–4919
48. de Graaf, K., Czajkowska, H., Rottmann, S., Packman, L. C., Lilischkis, R., Lüscher, B., and Becker, W. (2006) *BMC Biochem.* **7,** 7